

## Enhancement of Copper Antiviral Activity with Glutathione Treatment

Akiko Yamamoto,\* Masanori Kikuchi, and Yasushi Suetsugu

Cite This: *ACS Appl. Bio Mater.* 2026, 9, 5237–5248

Read Online

ACCESS |



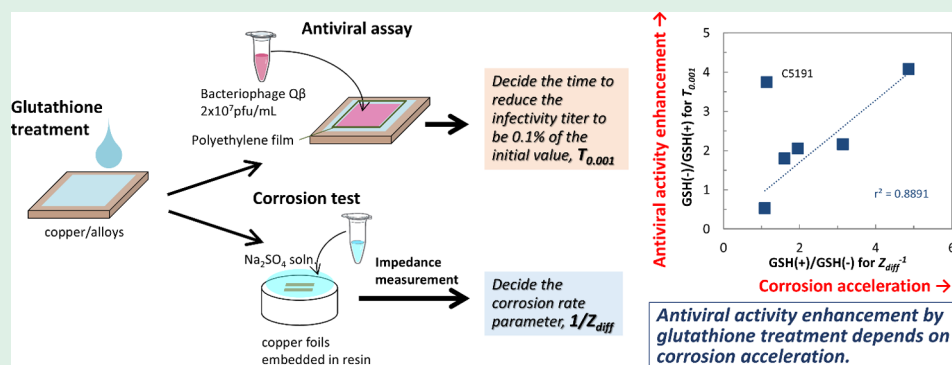
Metrics &amp; More



Article Recommendations



Supporting Information



**ABSTRACT:** Copper and its alloys have antimicrobial activity effective for various pathogens. Their application to touch surfaces successfully reduced bioburden in hospital intensive care units but failed to completely prevent the transmission of pathogens derived from the hospital room. Discoloration of pure copper with surface oxide growth is another issue to discourage its application to touch surfaces. Common copper alloys have relatively high resistance to discoloration, but their antimicrobial activity is lower than that of pure copper. Therefore, enhancement of the antimicrobial activity of copper alloys is beneficial for their touch surface application. In this study, glutathione was employed for surface treatment of copper and its alloys to enhance their antiviral activity. Treatment with 4 mM glutathione in 99 vol % ethanol–1% H<sub>2</sub>O markedly enhanced copper and its alloys' antiviral activities against bacteriophage Q $\beta$  except MONEL, which has the lowest Cu content (33.4 wt %). Electrochemical impedance measurement under a thin electrolyte film revealed acceleration of copper and its alloys' corrosion by the glutathione treatment. The antiviral activity of tested materials with the glutathione treatment correlated well with their corrosion rate, except MONEL. Potentiodynamic and chronopotentiometry measurements in 6 M KOH + 1 M LiOH demonstrated reduction in the thickness of the surface oxide layer by the glutathione treatment. These facts suggest that the glutathione treatment reduces the surface oxide layer, resulting in acceleration of corrosion with an increase in Cu ion release, which enhances antiviral activity.

**KEYWORDS:** antiviral tests, copper alloys, glutathione, electrochemical impedance spectroscopy, bacteriophage Q $\beta$

## 1. INTRODUCTION

Infection prevention and control is still one of the fundamental issues for hospitals and healthcare facilities. A risk of pathogen transmission is reported from a previously occupying patient via a hospital room.<sup>1</sup> To reduce this risk, sterilization of the room is attempted by irradiation of ultraviolet light or hydrogen peroxide vapor.<sup>2,3</sup> They are effective to reduce the infection of *Clostridioides difficile* or Vancomycin resistant *Enterococci* (VRE) in some degree, but failed to perfectly eliminate the infection derived from hospital rooms.<sup>2,4</sup> Therefore, there is still a need for the technologies to prevent the pathogen transmission via touch surfaces or other hospital environments.

Copper and its alloys are well-known to have antimicrobial activity, the so-called “contact killing”, which is continuously effective without energy supply for a variety of pathogens such as Gram-positive/-negative bacteria, fungi, and enveloped and nonenveloped viruses.<sup>5–8</sup> Therefore, many studies attempted

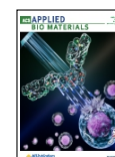
the application of copper and its alloys on hospital touch surfaces, demonstrating their successful reduction on bioburden in the hospital room as well as healthcare-associated infection (HAI).<sup>9–14</sup> Nine studies reported a significant reduction in total microbial burden on copper alloy surfaces from those on control surfaces (37–100% in reduction), and the meta-analysis of 3 studies resulted in the reduction of HAI by 26% (44 to 3% in a 95% confidential interval).<sup>10</sup> Though many clinical studies reported its success on bioburden reduction, the applica-

Received: March 18, 2026

Revised: May 11, 2026

Accepted: May 26, 2026

Published: June 3, 2026

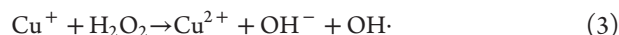
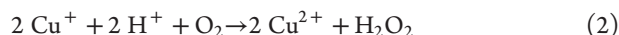


tion of copper and its alloys to high touch surfaces is still limited in numbers. One of the reasons may be discoloration of copper in ambient conditions. The metallic copper surface is covered by its oxides (a mixture of  $\text{Cu}_2\text{O}$  and  $\text{CuO}$ ), which keep growing in thickness, loosening the metallic copper appearance.<sup>15</sup> Copper alloys have better resistance against discoloration, but their antimicrobial activity depends on copper content in the alloy and is lower than that of pure copper.<sup>6,16</sup>

Another reason to discourage the application of copper and its alloys may be the reaction time of their antimicrobial activity in the real hospital environment. Generally, copper and its alloys require half an hour to several days to kill the microbes contacting to their surface depending on the conditions and types of microbes.<sup>5</sup> This is relatively faster than other antimicrobial materials (such as commercially available antimicrobial products made of resin containing antimicrobial reagents).<sup>16</sup> However, it may be not quick enough to prevent pathogen transmission via touch surfaces. Enhancement of the antimicrobial activity of copper and its alloys enables more efficient prevention of HAI via touch surfaces.

For the process of “contact killing” on a copper surface, the following 4 stages are proposed:<sup>5</sup> (1) corrosion of the copper surface with copper ion release, (2) depolarization and rupture of the cell membrane, (3) generation of reactive oxygen species (ROS) induced by copper ions, and (4) deoxyribonucleic acid (DNA) degradation. The importance of corrosion reaction and copper ion release is confirmed by the uptake and accumulation of copper ions inside the bacterial cells with the very fast reaction when contacting the copper surface.<sup>17</sup> Therefore, one of the strategies to improve the antimicrobial activity of copper materials is to increase their corrosion rate.

For the ROS generation involving copper ions, the following reactions (1–3) are suggested;<sup>5</sup>  $\text{Cu}^{2+}$  reacts with a sulfhydryl group (RSH), such as in cysteine or glutathione, transforming into  $\text{Cu}^+$ , which generates hydrogen peroxide ( $\text{H}_2\text{O}_2$ ) and hydroxyl radicals ( $\text{OH}\cdot$ ) by reacting with oxygen and  $\text{H}_2\text{O}_2$ , respectively.



The generation of  $\text{Cu}^+$  will increase ROS generation, causing severe damage to microbes. On the copper surface,  $\text{Cu}_2\text{O}$  is initially formed, followed by  $\text{CuO}$  at a longer exposure time.<sup>15,18</sup> This native oxide layer is not self-protective; oxidation continues at room temperature.<sup>15</sup> The water solubility of  $\text{CuO}$  is lower than  $\text{Cu}_2\text{O}$ , agreeing with the higher toxicity of the latter.<sup>18,19</sup> We hypothesized that an appropriate supply of the sulfhydryl substrate to the reaction place of copper with microbes should increase  $\text{Cu}^+$  to enhance antimicrobial activity.

Glutathione ( $\gamma$ -glutamylcysteinylglycine, abbreviated as GSH), is a low-molecular-weight tripeptide containing sulfhydryl groups. It is one of the common antioxidants widely distributed in plants, animals, and microbiomes.<sup>20</sup> The concentration of GSH leaches as high as 0.5–10 mM in animal cells,<sup>20</sup> suggesting its relatively low toxicity for humans. Therefore, we selected GSH as a sulfhydryl source.

In the present study, we investigated the surface treatment of pure copper and 5 kinds of copper alloys with GSH to enhance their antimicrobial activity focusing on the antiviral effect. We selected an alcohol–water solvent system as the treatment solution, emulating an alcohol disinfectant to be a simple and easy one, which enables repetitive application to copper high touch surfaces as needed. We decided to focus on antiviral activity against nonenveloped virus, bacteriophage Q $\beta$ , which is not destroyed by alcohol. Antiviral tests were performed following the Japanese Industrial Standard (JIS) R1706:2020,<sup>21</sup> which is the base document of updating ISO 18061:2014 “Fine Ceramics (Advanced Ceramics, Advanced Technical Ceramics)—Determination of antiviral activity of semiconducting photocatalytic materials—Test method using bacteriophage Q-beta”, without ultraviolet (UV)-light irradiation.

Electrochemical impedance measurement was also performed to investigate the effect of GSH treatment on corrosion of copper and its alloys. We selected this method to mimic the similar condition to bacteriophage Q $\beta$  application to the copper surface, under a thin solution layer. Based on the obtained results, the correlation between corrosion acceleration and antiviral activity enhancement by GSH treatment was discussed.

## 2. MATERIALS AND METHODS

### 2.1. Testing Materials

Materials used were oxygen-free copper (C1020) and 5 kinds of copper alloys (C5191, C7150, C2680, Constantan, and MONEL400). Their chemical compositions are described in Table S1. The foils (0.03–0.1 mm in thickness) of these materials were purchased from the Nilaco Corporation (Tokyo, Japan). All materials were cut into 20 mm squares for an antiviral assay. Prior to the assay, the specimen surfaces were cleaned with a detergent (a mixed solution of sodium  $\alpha$ -dodecan-1-yl- $\omega$ -(sulfonatoxy)poly(oxyethylene) and fatty acid alkanolamide), followed by rinsing thoroughly with running ultrapure water and air-drying. The bottom surface of each specimen was covered with a thin silicone film (0.1 mm, AS ONE, Osaka, Japan) to avoid the contact to the collecting solution of surviving viruses. The top surface was cleaned with a lint-free wiper containing absolute ethanol (abbreviated as EtOH, ethanol 99.5, guaranteed reagent, FUJIFILM Wako Pure Chemical, Osaka, Japan).

For electrochemical impedance spectroscopy, the copper and alloy foils of 0.1 mm thickness were cut into pieces of 10 mm width and 15 mm length. One side of the foil was covered by a 50  $\mu\text{m}$ -thick polyimide insulating tape (PIA220, 3 M Japan, Tokyo, Japan). Then, two pieces of the same material were layered with the covered side facing inward and were vertically embedded into low-viscosity resin (27–777, Refine Tech, Yokohama, Japan) using a round mold with a 25.4 mm diameter. The two cross sections of 10 mm length and 0.1 mm width appeared on the resin top surface in parallel with a gap of 0.1 mm, as shown in Figure S1. The specimen surface was polished by SiC paper up to #1200, followed by rinsing thoroughly with running ultrapure water and air-drying. The periphery of the resin was covered by the insulating tape making a rim of 0.5 mm in height. Prior to glutathione treatment (described in the following paragraph), the specimen top surface was plasma-treated with a hydrophilic treatment device (HDT-400, JEOL DATUM, Tokyo, Japan) for 120 s at a diamond knife mode to help the wetting of resin with a glutathione solution.

### 2.2. Surface Treatment with Glutathione

Glutathione (reduced form, Wako Special Grade, abbreviated as GSH) was purchased from FUJIFILM Wako Pure Chemical. A 0.123 g portion of GSH was dissolved with 1 mL of ultrapure water to prepare 400 mM solution. Then, an appropriate portion of the 400 mM

GSH solution was mixed with ethanol and ultrapure water to prepare 1, 2, and 4 mM GSH in 1 vol % H<sub>2</sub>O–99 vol % EtOH or 4 mM GSH in 99–80 vol % EtOH. Since GSH is not soluble into EtOH, 4 mM is the maximum concentration in 99 vol % EtOH absent of precipitation. The GSH solution was prepared on the same day of applying to the specimen surface.

Each of the specimens for the antiviral assay was placed on the bottom of a glass dish individually. Then, a 5  $\mu$ L portion of the GSH treatment solution was poured and spread on the specimen surface using a micropipette tip. Since the specimen was a 20 mm square, the hypothetical thickness of the GSH solution spread on the specimen surface was calculated as 1.25  $\mu$ m. Due to its high ethanol content, the applied portion of the treatment solution was promptly dried within 5 min at ambient temperature. Then, the specimen was placed in the safety cabinet at ambient temperature for certain periods of time (1, 3, 24, and 168 h) prior to the antiviral test.

For electrochemical impedance measurement, a 13  $\mu$ L portion of the 4 mM GSH in 99 vol % EtOH was poured and spread on each specimen (parallel electrodes embedded in resin) immediately after its hydrophilic treatment using a micropipette tip. Since the specimen diameter was 25.4 mm, the hypothetical thickness of the GSH solution spread on the specimen surface was calculated as 2.57  $\mu$ m. The specimen was air-dried at ambient temperature overnight prior to the electrochemical impedance measurement.

### 2.3. Antiviral Assay Using Bacteriophage Q $\beta$

The procedure of the antiviral assay is schematically shown in Figure S2. The assay is based on the JIS R1706:2020<sup>21</sup> without irradiation of UV light. Bacteriophage Q $\beta$  (NBRC20012) and its host bacterium, *Escherichia coli* (*E. coli*, NBRC106373), were obtained from the National Institute of Technology and Evaluation (Tokyo, Japan) and prepared with the following protocols<sup>21</sup> as briefly described below. Experiments were performed in duplicate.

**2.3.1. Preparation of Bacteriophage Stock Suspension.** A portion of stored *E. coli* on agar slants of Luria–Bertani (LB) broth (LB agar “DAIGO”, SHIOTANI M.S., Amagasaki, Japan) was added to calcium-containing LB (CaLB), which contains 9.9 g/L peptone, 5.0 g/L yeast extract, 9.9 g/L NaCl, and 0.29 g/L CaCl<sub>2</sub>·2H<sub>2</sub>O, prepared by addition of CaCl<sub>2</sub>·2H<sub>2</sub>O (guaranteed reagent, FUJIFILM Wako Pure Chemical) to LB (LB broth “DAIGO”, SHIOTANI M.S.). The bacterial suspension was cultured at 37 °C with shaking at 110  $\pm$  10 rpm for 18  $\pm$  2 h. Then, a portion of this bacterial suspension was transferred into the new batch of CaLB at the ratio of 1/1000 and cultured at the same condition to obtain the bacterial density of 2  $\times$  10<sup>8</sup> cfu/mL (reaching an absorbance of ca. 0.12 at 650 nm with a 0.63 cm path length). Then, bacteriophage Q $\beta$  was added to the bacterial suspension to be roughly 1/10 of the bacteria, that is, ca. 2  $\times$  10<sup>7</sup> pfu/mL. It was cultured at the conditions previously described for 4 h. Then, the bacteriophage-infected bacterial suspension was transferred and stored overnight in the fridge (4 °C). The solution was centrifuged at 10,000 g for 20 min at 4 °C. The supernatant was collected and filtered through a membrane filter with a pore size of 0.22  $\mu$ m (DISMIC-25SS, ADVANTEC TOYO KAISHA, Tokyo, Japan) and stored at –80 °C. The virus infectivity titer was decided prior to the antiviral assay.

**2.3.2. Preparation of *E. coli* for the Plaque Assay.** A portion of stored *E. coli* was added into CaLB and cultured for 20  $\pm$  4 h at 37 °C. Then, this bacterial suspension was transferred into a new batch of CaLB at the ratio of 1/10 and cultured for 6–7 h at 37 °C to obtain the bacterial density of 0.5–2.0  $\times$  10<sup>9</sup> cfu/mL (reaching an absorbance of ca. 0.4 at 650 nm with a 0.63 cm path length).

**2.3.3. Preparation of Bacteriophage Loading Suspension and Application.** The stock suspension of the bacteriophage Q $\beta$  was appropriately diluted with a 500-fold dilution of nutrient broth (NB “Eiken”, Eiken Chemical, Tokyo, Japan), which is abbreviated as 1/500 NB thereafter, to be an expected infective titer of 0.67–2.6  $\times$  10<sup>7</sup> pfu/mL. The 1/500 NB contained 0.006 g/L meat extract,

0.02 g/L peptone, and 0.01 g/L NaCl. Then, the loading suspension was stored at 0 °C and used within 2 h.

A 50  $\mu$ L portion of the bacteriophage suspension in 1/500 NB was placed onto a specimen surface and covered by a polyethylene film (0.04 mm, UNIPACK, SEISANNIPPONSHA, Tokyo, Japan) of 12 mm square, which was cleaned by EtOH in advance. A bottom of a clean, sterile glass dish was used as a control surface. The specimen was placed for certain time periods (5, 10, and 20 min) in the safety cabinet at ambient temperature. Then, the bacteriophages on the specimen surface were collected into 1 mL of soybean-casein digest broth with lecithin and polyoxyethylene sorbitan monooleate (abbreviated as SCDLB broth, SHIOTANI M.S.), which contained 17 g/L casein, 3.0 g/L soybean peptone, 5.0 g/L NaCl, 2.5 g/L Na<sub>2</sub>HPO<sub>4</sub>, 2.5 g/L glucose, 1.0 g/L lecithin, and 7.0 g/L nonionic surfactant, by pipetting. Then, the collected solution was stored at 0 °C before the quantification of virus infectivity titer by the plaque assay.

**2.3.4. Quantification of Virus Infective Titer by the Plaque Assay.** The collected solution was serially diluted by a 10-fold manner with physiological saline containing 0.1 wt % peptone (abbreviated as pepNaCl), which contains 1.0 g/L peptone (Kyokuto peptone, Kyokuto Pharmaceutical Industrial, Tokyo, Japan) and 8.5 g/L NaCl (guaranteed reagent, FUJIFILM Wako Pure Chemical). The aliquots of collected and diluted solutions were individually added to 0.1 mL of *E. coli* prepared for the plaque assay, mixed, and warmed at 37 °C for 10 min. Then, the suspension containing bacteria and bacteriophage was mixed with a 4 mL portion of CaLB soft agar (agar concentration of 0.5 wt %), which was maintained at 55 °C, well-pipetted, and layered over a CaLB agar (agar concentration of 1.5 wt %) dish warmed at 37 °C. After solidification at ambient temperature in a safety cabinet, the multilayered agar dishes were incubated for 18  $\pm$  2 h at 37 °C prior to counting plaques.

The virus infectivity titer, *N* (pfu/mL), was decided by the following equation:

$$N = A \times D_F \times (1/V)$$

where *A* indicates the average number of plaques in the duplicated dishes at the same dilution and *D<sub>F</sub>* describes dilution factor. *V* represents the volume (mL) of the collected or diluted bacteriophage solutions added to *E. coli* suspension.

Two parameters for antiviral activity were introduced: *T*<sub>0.001</sub> and minimum inhibitive contact time (MICT). The former is the contact time to reduce *N* on the specimen surface (*N*<sub>mat</sub>) to 1/1000 of that on the control surface (*N*<sub>cont</sub>). The latter is the contact time when *N*<sub>mat</sub> becomes zero. *T*<sub>0.001</sub> was determined by probit regression on *N*<sub>mat</sub>/*N*<sub>cont</sub> against the logarithm of contact time. When probit regression was not applicable, *T*<sub>0.001</sub> was estimated by linear regression on the logarithm of *N* of the inoculated phages (at contact time zero) and the logarithm of *N*<sub>mat</sub> (=0) at contact time *S*. MICT was estimated by linear regression on the logarithm of *N*<sub>mat</sub> against the logarithm of contact time.

### 2.4. Electrochemical Impedance Analysis

In order to investigate the effect of GSH treatment on the corrosion of copper and its alloys, electrochemical impedance spectroscopy (EIS) under a thin electrolyte layer was performed. This method enables us to mimic the contact condition of bacteriophage on the specimen surface in the antiviral assay; a small quantity (50  $\mu$ L) of bacteriophage suspension was placed on the specimen surface with the polyethylene film cover to form a thin layer. The ratio of the solution amount to specimen surface area is one of the key factors to influence the corrosion behavior of testing materials.

The experimental procedures were described in our previous study,<sup>22</sup> which uses a specimen having parallel electrodes of testing materials as described earlier (Figure S1). Briefly, 0.5 mL of 0.7 M Na<sub>2</sub>SO<sub>4</sub> (guaranteed reagent, FUJIFILM Wako Pure Chemical) was applied on the specimen surface with/without GSH treatment, giving



a salt density of 9.8 mg/cm<sup>2</sup>. The specimen was placed in the incubator (25 ± 1 °C), and EIS measurement was immediately started with an AC amplitude of 10 mV in the frequency range of 1 × 10<sup>-2</sup> to 2 × 10<sup>4</sup> Hz using a potentiostat equipped with a frequency response analyzer (Interface 1010 T, Gamry Instruments, Warminster, USA). This result in the electrolyte was indicated as 100% humidity. Then, the humidity in the incubator was controlled to be 30 ± 5% relative humidity (RH) using silica gel overnight to dry the moisture. EIS was performed the next day, followed by the increases in the humidity to 60 ± 5, 75 ± 5, and 90 ± 5% RH by controlling the open surface area of ultrapure water in a vessel in the incubator. EIS measurement was started 0.5 h after the relative humidity of the incubator reached to the designated range. The humidity in the incubator was monitored with a hygrometer (Weathecom II electronic thermos and hygrometer EX-502, EMPEX Instruments, Tokyo, Japan) through the measurement.

The EIS data were analyzed with an equivalent circuit shown in Figure S3.<sup>23</sup> The difference between the impedances at high (20 kHz) and low (10 mHz) frequency ranges was calculated as  $Z_{\text{diff}}$  and its reciprocal number ( $1/Z_{\text{diff}}$ ) was employed as a corrosion parameter. This parameter was introduced as a practical solution for corrosion monitoring by impedance measurement under a thin electrolyte layer without curve fitting.<sup>23,24</sup> It gives a reasonable accuracy for the relative comparison of the corrosion behavior of testing materials in different conditions.<sup>23,24</sup> Details of the calculation procedure and relevance of  $1/Z_{\text{diff}}$  are described in the Supporting Information. EIS measurements were performed in triplicate.

## 2.5. Electrochemical Analysis of the Oxide Layer Formed on the Copper Surface

In order to analyze the effect of GSH treatment on the oxide layer of the copper surface, potentiodynamic (PD) and chronopotentiometric (CP) measurements were carried out in the highly alkaline solution.<sup>25</sup> As a testing specimen, a thin plate of C1020 with a thickness of 0.3 mm was cut into 15 mm squares and used as received. Prior to the measurement, 5.6 μL of 4 mM GSH in 99 vol % EtOH was applied to the specimen and kept for 24 h in the ambient condition, if necessary. Then, the testing specimen was placed at the bottom of an electrochemical chamber with an exposed area of 0.899 cm<sup>2</sup> as a working electrode. A platinum wire was set as a counter electrode, whereas a saturated Ag/AgCl (3 M NaCl) electrode was used as a reference electrode. A 27 mL portion of 6 M KOH + 1 M LiOH,<sup>25</sup> which was prepared by appropriate dilution of 8 M KOH and 4 M LiOH (both for volumetric analysis, FUJIFILM Wako Pure Chemical), was employed as an electrolyte. For PD measurement, a potential was swept from the open-circuit potential (~ -0.6 V vs Ag/AgCl) to that for hydrogen evolution (-1.6 V vs Ag/AgCl) at the rate of 1.0 mV/s. For CP measurement, the current density was set as 0.1 mA/cm<sup>2</sup> while recording potential against the reference electrode at the sampling rate of 0.1 s.

The thickness of oxides [Cu(OH)<sub>2</sub>, Cu<sub>2</sub>O, and CuO] was determined based on the results of CP measurement following the procedure in the literature,<sup>26</sup> and the details are described in the Supporting Information. The PD and CP measurements were performed in triplicate.

## 2.6. Statistical Analysis

For the results of the antiviral assay, parallelism tests of 2 regression lines were performed using a free version of statistical analysis software (Kypplot 6.0, KyensLab, Japan) except some cases; the pairs of the virus infectivity titer with/without GSH treatment at a contact time of 5 or 10 min were analyzed by Student's *t*-test. The analysis methods applied are listed for the combination of different surface treatment solutions and different materials in Table S2.

For the results of EIS measurement, the pairs of the  $1/Z_{\text{diff}}$  values of the same material with/without GSH treatment were analyzed by Student's *t*-test. For the CP analysis, the pairs of the oxide thickness for the same materials with/without GSH treatment were analyzed by Student's *t*-test.

In all experiments, the rejection of the obtained values was decided by Dixon's *Q*-test at 90% confidence.

## 3. RESULTS

### 3.1. Effect of Glutathione Treatment on the Antiviral Activity of Copper and Its Alloys

The effect of GSH treatment on the antiviral activity of C1020 is shown in Figure 1a. At 24 h after the treatment, the *N* of C1020 treated with 4 mM GSH in 99 vol % EtOH (abbreviated as 4 mM GSH<sub>99</sub> in the following) was decreased to zero just after 5 min of contact, whereas that of nontreated C1020 was around 10<sup>5</sup> pfu/mL after 5 min of contact and was not decreased to zero even after 20 min of contact. C1020 treated only with 99 vol % EtOH (without GSH) had a similar result to that of nontreated C1020. These results clearly demonstrate the enhancement effect of GSH treatment on the antiviral activity of C1020. Figure 1a also shows that the *N* of glass treated with 4 mM GSH<sub>99</sub> was reduced to 3.9 × 10<sup>5</sup> pfu/mL, which is slightly lower than that of glass treated only with 99 vol % EtOH. However, both *N* values for glass treated with 99 vol % EtOH with/without GSH did not decrease further with an increase in contact time. This indicates that nontreated C1020 had higher antiviral activity than glass with GSH treatment and that GSH treatment did not work on glass in the similar level to that on C1020, suggesting the involvement of Cu ions in the enhancement process of antiviral activity by GSH treatment. C1020 treated with 4 mM GSH<sub>99</sub> had a statistically different regression line from those of C1020 treated only with 99 vol % EtOH, nontreated C1020, and glass treated with 99 vol % EtOH with/without GSH (*p* < 0.001).

The effects of the EtOH/water ratio and GSH concentration in the treatment solution on the enhancement of antiviral activity of C1020 are shown in Figure 1b and Figure S4, respectively. At 24 h after the treatment, the reduction in EtOH concentration in the treatment solution increased *N*, indicating the reduction in antiviral activity (Figure 1b). The decrease in GSH concentration increased *N* of C1020 (Figure S4), suggesting the best treatment solution among those tested in this study as 4 mM GSH<sub>99</sub>. In both experiments, C1020 treated with 4 mM GSH<sub>99</sub> has a statistically different regression line from that treated with 4 mM GSH in 95 vol % or 80 vol % EtOH (*p* < 0.001) and from that treated with 2 or 1 mM GSH in 99 vol % EtOH (*p* < 0.001).

The duration of the enhancing effect by GSH treatment was evaluated using C1020 at the contact times of the phage suspension as 5 and 10 min, as shown in Figure S5. At the contact time of 5 min, the *N* of GSH-treated C1020 reached to zero at up to 24 h after the treatment, but it increased to about 10<sup>3</sup> pfu/mL at 168 h (=7 days) after the treatment. However, at the contact time of 10 min, *N* was still zero even at 168 h after the treatment. These results indicated that the GSH treatment maintained its maximum effectiveness up to 24 h after the treatment and that its enhancement effect remained in a practical level even at 168 h after the treatment. In both contact times, the *N* of nontreated C1020 was significantly higher than that of GSH-treated C1020 at all leaving time points after the treatment (*p* < 0.01).

Figure 2 indicates the effect of GSH treatment on antiviral activity of copper alloys with various Cu contents. C7150, a

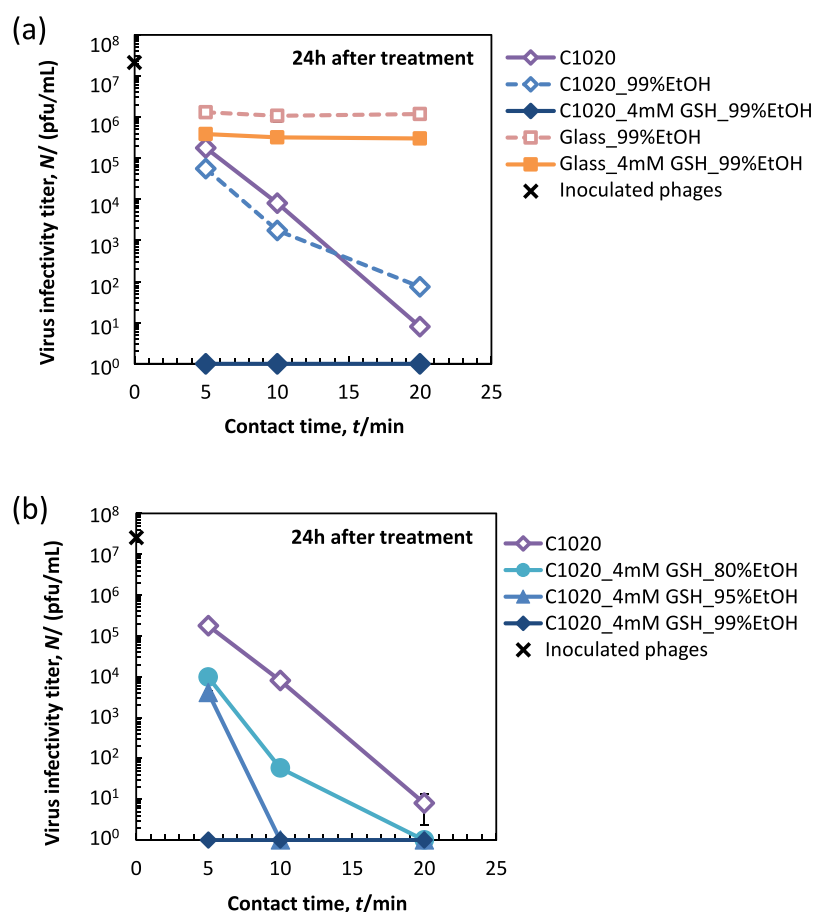


**Figure 1.** Effect of GSH treatment (a) and ethanol concentration (b) on antiviral activity of C1020 at 24 h after the treatment ( $n = 2$ , mean  $\pm$  s.d.). By parallelism tests of 2 regression lines, C1020 treated with 4 mM GSH in 99 vol % EtOH has a statistically different slope from that of C1020 treated only with 99 vol % EtOH or nontreated one ( $p < 0.001$ ). C1020 treated with 4 mM GSH has a statistically different intercept from that of glass treated with 99 vol % EtOH with/without 4 mM GSH ( $p < 0.001$ ). C1020 treated with 4 mM GSH in 99 vol % EtOH has a statistically different slope from that treated with 4 mM GSH in 95 vol % or in 80 vol % EtOH ( $p < 0.001$ ). Nontreated C1020 has a statistically different slope from that treated with 4 mM GSH in 95 vol % or in 80 vol % EtOH ( $p < 0.001$  or  $p < 0.05$ , respectively).

Cu-30 wt % Ni alloy, showed superior antiviral activity without treatment as  $N$  leached to zero at 10 min of contact. GSH treatment to C7150 resulted in a zero value of  $N$  at 5 min of contact, indicating the enhancement effect of the GSH treatment on its antiviral activity. Nontreated C5191, C2680, and Constantan had similar antiviral activity to that of C1020. GSH treatment to these alloys decreased their  $N$  values, but not as low as GSH-treated C1020. GSH treatment to MONEL slightly reduced  $N$ , especially at the shorter contact time, but the values are much higher than other copper alloys, indicating less effectiveness of the GSH treatment on antiviral activity enhancement. For C5191, C2680, Constantan, and MONEL, the GSH treatment significantly changed their antiviral behavior, which is confirmed by parallelism tests for 2 regression lines ( $p < 0.001$  for C5191, C2680, and Constantan,  $p < 0.01$  for MONEL).

Two parameters of the antiviral activity,  $T_{0.001}$  and MICT, were calculated for each testing material and are shown in Table 1. Without GSH treatment, the smallest  $T_{0.001}$  and MICT values were observed for C7150, followed by C1020.  $T_{0.001}$  and MICT values tended to increase with a decrease in Cu content in the alloys except C7150. With GSH treatment, the trends in  $T_{0.001}$  and MICT were similar to those without GSH treatment; the smallest values were observed for C7150

and C1020, followed by C5191, and increased with a decrease in Cu content in the alloys.

### 3.2. Effect of GSH Treatment on the Corrosion of Copper and Its Alloys

The examples of the electrochemical impedance spectra of C1020 with/without GSH treatment under various humidity are shown in Figure S6. In both cases, the impedance increased with reduction in humidity. As a corrosion parameter,  $1/Z_{\text{diff}}$  was calculated and is plotted against humidity in Figure 3a. It indicates the increasing trend in  $1/Z_{\text{diff}}$  by GSH treatment at the humidity range of over 75% RH.

The  $1/Z_{\text{diff}}$  values of all materials with/without GSH treatment at 100% and 90% RH are shown in Figures 3b and 3c, respectively. At 100%,  $1/Z_{\text{diff}}$  of GSH-treated materials tended to be higher than those of nontreated, indicating the increase in the corrosion rate by GSH treatment. In addition,  $1/Z_{\text{diff}}$  also tended to decrease with reduction in Cu content in the materials. However, the difference in  $1/Z_{\text{diff}}$  with/without GSH treatment decreased with reduction in humidity (see Figure 3a). Even at 90% RH, there is no difference in  $1/Z_{\text{diff}}$  between materials and with/without GSH treatment except C1020 and C5191 (Figure 3c).

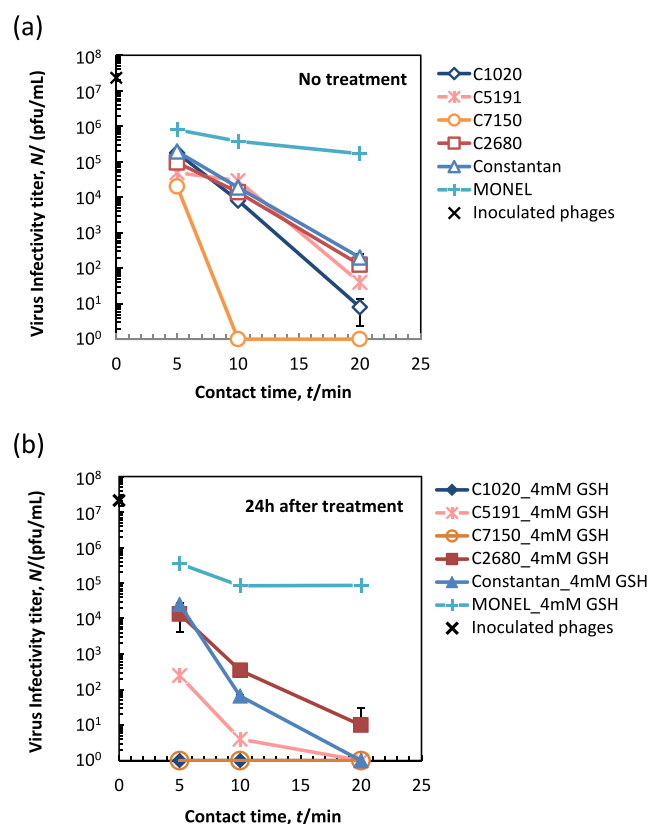


**Figure 2.** Antiviral activity of common copper alloys with/without GSH treatment ( $n = 2$ , mean  $\pm$  s.d.). By parallelism tests of 2 regression lines, C1020, C5191, or Constantan treated with 4 mM GSH has a statistically different slope from the corresponding nontreated material ( $p < 0.001$ ). C2680 or MONEL treated with 4 mM GSH has a statistically different intercept from the corresponding nontreated material ( $p < 0.001$  or  $p < 0.01$ , respectively). The parallelism test was not applicable to the data of C7150.

### 3.3. Correlation between Antiviral Activity and Corrosion of Copper and Its Alloys

In order to investigate the correlation between the antiviral activity and corrosion rate of testing materials, the  $T_{0.001}$  and MICT of the testing materials treated with/without GSH were plotted against  $1/Z_{\text{diff}}$  at 100% RH (in an electrolyte) in logarithmic scales as shown in Figure 4a. The  $1/Z_{\text{diff}}$  of the nontreated materials showed no clear trend, but those of the

GSH-treated ones indicated a good linear correlation to  $T_{0.001}$  except MONEL ( $r^2 = 0.934$ ). The similar trend was observed for the correlation between the  $1/Z_{\text{diff}}$  and MICT for the GSH-treated materials except MONEL ( $r^2 = 0.971$ , Figure S7a). These results suggest that the GSH treatment-induced higher corrosion rate in the electrolyte resulted in the higher antiviral activity of the testing materials except MONEL, which has a relatively low Cu content (33.4 wt %).

In order to investigate the enhancement level of antiviral activity by the GSH treatment in relation to acceleration in the corrosion rate, the ratio of the  $T_{0.001}$  of testing materials treated with/without GSH [abbreviated as GSH(+) and GSH(-), respectively] were plotted against that of the  $1/Z_{\text{diff}}$ . For the  $T_{0.001}$  and MICT, in which the smaller values indicate the higher antiviral activity, the larger values of GSH(-)/GSH(+) indicate the higher levels in enhancement of the antiviral activity. For the  $1/Z_{\text{diff}}$  in which the larger values indicate the higher corrosion rate, the larger values of GSH(+)/GSH(-) indicate the higher levels of acceleration in the corrosion rate. As shown in Figure 4b, the GSH(-)/GSH(+) of the  $T_{0.001}$  linearly increased with an increase in the GSH(+)/GSH(-) of the  $1/Z_{\text{diff}}$  except C5191 ( $r^2 = 0.889$ ). The same trend was also observed for MICT as  $r^2 = 0.927$  (Figure S7b). These trends suggested that the enhancement in antiviral activity depended on the corrosion acceleration of testing materials by the GSH treatment.

### 3.4. Effect of Glutathione Treatment on the Oxide Layer of the Copper Surface

In order to investigate the effect of GSH treatment on the naturally formed oxide layer of the copper surface, PD and CP measurements were carried out under the condition previously reported as effective to identify  $\text{Cu}_2\text{O}$  and  $\text{CuO}$ .<sup>25</sup> The typical examples of the measurements for C1020 with/without GSH treatment are displayed in Figure 5. In the results of PD measurement (Figure 5a), the C1020 specimen shows a sharp peak around  $-0.7$  V vs Ag/AgCl and a very small peak around  $-1.2$  V vs Ag/AgCl, which can be assigned to  $\text{Cu}(\text{OH})_2$  and  $\text{CuO}$ , respectively.<sup>27</sup> This result corresponds well to the corrosion process of the copper plate in the laboratory air;  $\text{Cu}(\text{OH})_2$  is first formed and eventually converted to  $\text{CuO}$ .<sup>27</sup> Then,  $\text{Cu}_2\text{O}$  is formed after a certain period of time ( $\sim 10$  days),<sup>27</sup> but it was not clearly observed in our specimens. The C1020 specimen with GSH treatment had a smaller peak around  $-0.7$  V vs Ag/AgCl and no peak around  $-1.2$  V vs Ag/AgCl, suggesting less oxide layer on the specimen surface.

**Table 1.** Time to Reduce the Infectivity Titer of the Bacteriophage to 1/1000 of the Control Surface ( $T_{0.001}$ , min) and Minimum Inhibitive Contacting Time (MICT, min) of Testing Materials with/without GSH Treatment

material	Cu content (wt %)	Ni content (wt %)	$T_{0.001}$ (min)		MICT (min)	
			no treatment	24 h after GSH treatment	no treatment	24 h after GSH treatment
C1020	100		11.7	<2.88 <sup>a</sup>	22.9	<5
C5191	93.3		15.2	4.05	28.1	12.6
C7150	68.8	30.1	6.48	<3.00 <sup>a</sup>	10	<5
C2680	65.0		16.8	9.36	30.9	31.0
Constantan	54.4	44.6	15.7	7.64	31.5	16.3
MONEL	33.4	64.7	122	230	5910 <sup>b</sup>	9040 <sup>b</sup>

<sup>a</sup> $T_{0.001}$  was estimated by the linear regression of the logarithm of the virus infectivity titer values against contact time. <sup>b</sup>MICT was estimated by the probit method.

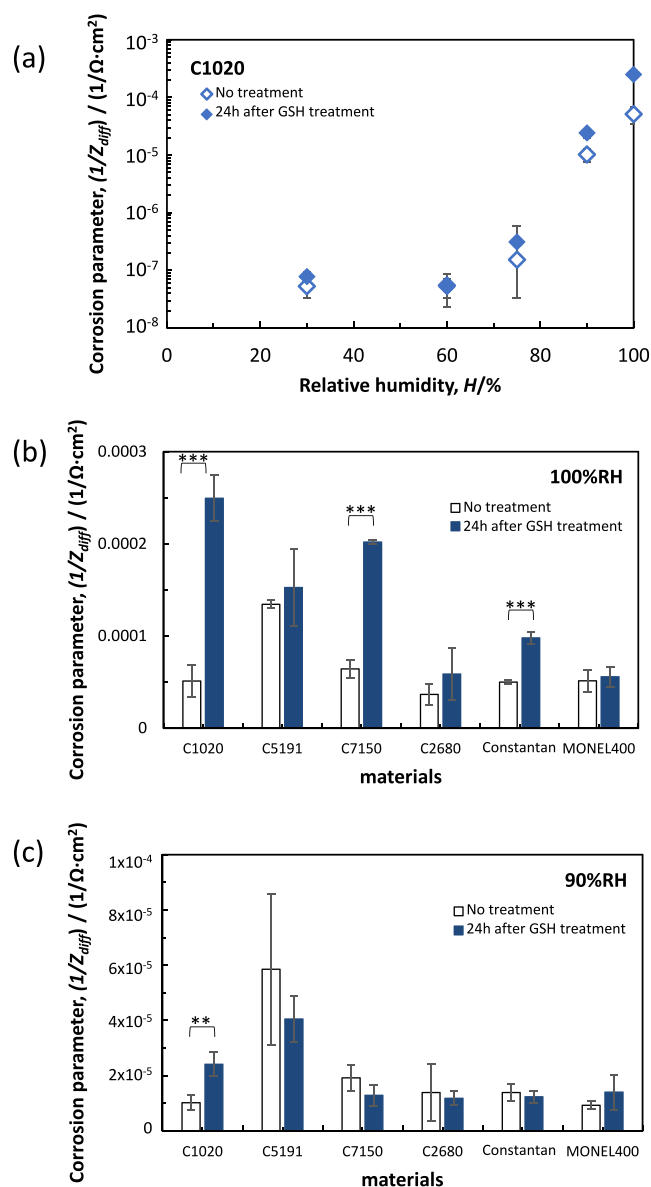


**Figure 3.** Results of electrochemical impedance measurement on C1020 under controlled humidity (a) and enhancement in the corrosion rate of copper alloys by GSH treatment in an electrolyte (100% RH, b) and that under 90% RH (c) ( $n = 3$ , mean  $\pm$  s.d.). The pairs of the  $1/Z_{diff}$  values of nontreated and treated materials were analyzed by Student's  $t$ -test.  $^{**}p < 0.01$ ,  $^{*}p < 0.001$ .

This can be attributed to the reduction activity of GSH applied to the surface. This decrease in the surface oxide was also confirmed by the CP measurement shown in Figure 5b. The nontreated C1020 surface had the retention of potentials around  $-0.7$  and  $-1.2$  V vs Ag/AgCl, corresponding to the reduction of  $\text{Cu}(\text{OH})_2$  and  $\text{CuO}$ , respectively. It also showed a very small additional potential drop around  $-1.4$  V vs Ag/AgCl assigned to the reduction of  $\text{Cu}_2\text{O}$ . The GSH-treated C1020 had similar behavior, with the potential retention around  $-0.7$  and  $-1.2$  V vs Ag/AgCl, but their duration was shorter than that of nontreated C1020, indicating that the oxide layer on the GSH-treated C1020 was thinner than that on nontreated. Table 2 shows the estimated thickness of  $\text{Cu}(\text{OH})_2$ ,  $\text{CuO}$ , and  $\text{Cu}_2\text{O}$

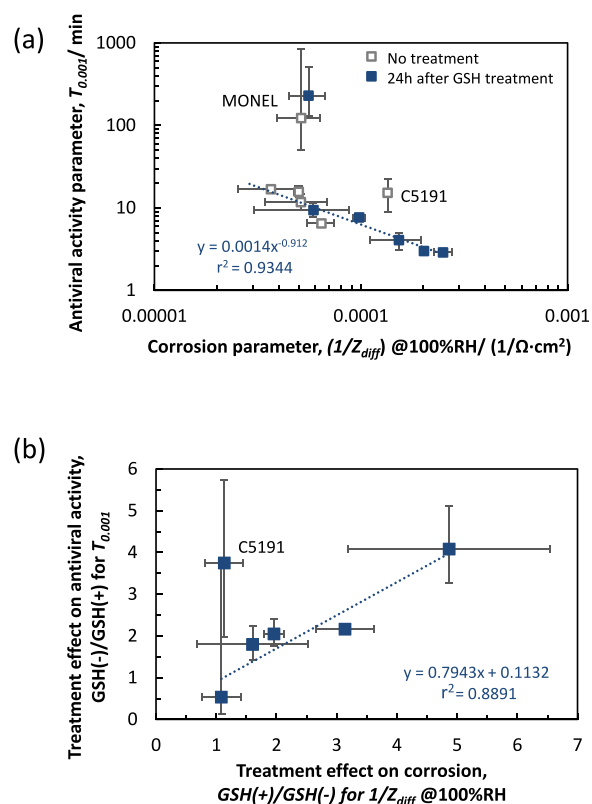


**Figure 4.** Correlation between the antiviral activity and corrosion rate of copper and its alloys (a) and correlation in the enhancement levels of antiviral activity and those of the corrosion rate by GSH treatment (b). GSH(+) and GSH(−) indicate with/without GSH treatment. The regression line shown in (a) was calculated for the 5 data with GSH treatment except MONEL. The regression line shown in (b) was calculated for the 5 data except C5191. The error bars in X and Y axes indicate standard deviations and 95% confidential intervals, respectively.

for C1020 with/without the GSH treatment based on the results of CP measurement. This clearly indicated the reduction in  $\text{Cu}(\text{OH})_2$  layer thickness after the GSH treatment ( $p < 0.1$ ). The thicknesses of  $\text{CuO}$  and  $\text{Cu}_2\text{O}$  were slightly increased and decreased with the GSH treatment, respectively, but their differences from those on C1020 without the treatment were not statistically significant.

#### 4. DISCUSSION

Copper and its alloys are well-known to have antimicrobial activity effective for a wide range of pathogens. It is ideal to test developed materials with every kind of pathogen, but it is not practical. Usually, representative ones are employed as the screening tests of the developed materials. The general order of resistance of microbes to disinfectants and sterilants is proposed as follows: prions > bacterial spores > parasitic oocysts > mycobacteria > nonenveloped viruses > fungal spores > vegetative fungi > vegetative bacteria > enveloped viruses.<sup>28</sup> It is preferable to use the most resistant pathogen for the efficacy tests, but it also gives the higher biological risk requiring the higher level of safety equipment. In the present study, a nonenveloped virus, bacteriophage Q $\beta$ , which can be handled in a BSL1 laboratory, was employed for antiviral activity evaluation since it is not destroyed by ethanol. As described earlier,



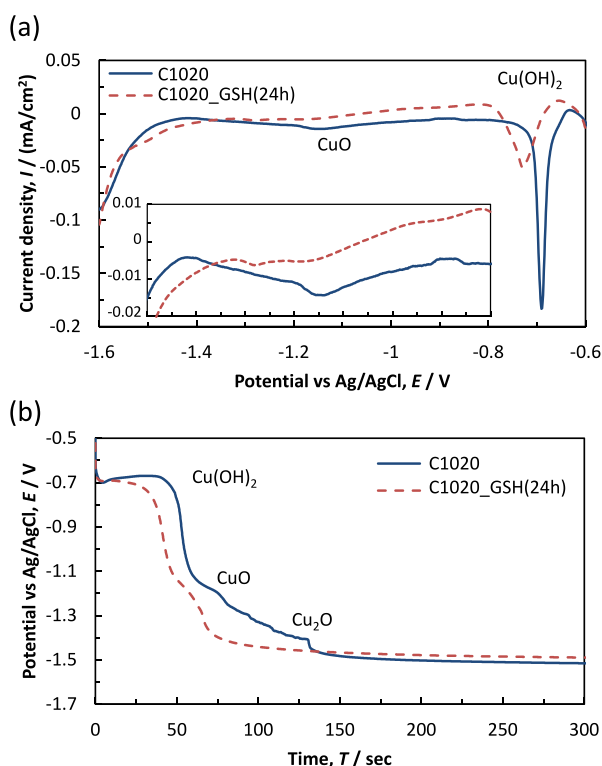


**Figure 5.** Typical examples from the results of (a) potentiodynamic and (b) chronopotentiometric measurements of C1020 specimens with/without GSH treatment.

**Table 2. Surface Oxide Thickness (nm) Estimated by Chronopotentiometric Measurements of C1020 with/without GSH Treatment ( $n = 3$ , Mean  $\pm$  s.d.)**

	no treatment	GSH treatment
Cu(OH) <sub>2</sub>	11.31 $\pm$ 1.55 <sup>a</sup>	8.86 $\pm$ 0.41 <sup>a</sup>
CuO	1.80 $\pm$ 0.38	2.87 $\pm$ 1.30
Cu <sub>2</sub> O	5.17 $\pm$ 2.53	1.22 $\pm$ 0.03

<sup>a</sup>A statistically significant difference was observed between “no treatment” and “GSH treatment” by Student’s *t*-test ( $p < 0.1$ ).

bacteriophage Q $\beta$  is assigned as a testing virus for antiviral tests of fine ceramics by JIS R1706:2020,<sup>21</sup> which is the base document of updating corresponding ISO 18061:2014. Nonenveloped viruses are not the highest pathogens in the resistance hierarchy but are higher than fungi, vegetative Gram-positive/negative bacteria, and enveloped viruses, expecting that the materials having the sufficient antiviral activity against nonenveloped viruses would be effective against these pathogens. This approach is acceptable for the screening stage of antimicrobial materials, but it is necessary to test the materials with target pathogens on the final stage of the development process.

As shown in Figure 2, the GSH treatment enhanced the antiviral activity of copper and its alloys. Although the enhancement was unclear on MONEL having the lowest Cu content as 33.7 wt %, it was clearly higher on C5191, C2680, and Constantan in comparison to nontreated C1020. The antimicrobial activity of copper alloys generally depends on their Cu

content.<sup>6,16</sup> C1020, which has the highest antimicrobial activity among copper materials, is most frequently studied on touch surface application, but its practical application is limited by discoloration. Common copper alloys such as C2680 have better resistance against discoloration, but their antimicrobial activity is lower than that of C1020. Therefore, enhancement of their antiviral activity by the simple GSH treatment would be a good practical solution to this issue.

Most of the studies on enhancement of copper antimicrobial activity use copper salts, oxides, nanoparticles (NPs), or nano-clusters (NCs) with a combination to a certain type of organic compound.<sup>29–34</sup> GSH is commonly employed for the synthesis of copper NPs and NCs as a capping agent since the thiol group in GSH has high affinity to copper,<sup>29</sup> resulting in inhibition of aggregation or growth of NPs/NCs. In some cases, GSH is also used as a reducing agent, but in other cases, typical reducing agents such as ascorbic acid, chitosan, citrate, hydrazine, and sodium borohydride are added.<sup>29</sup> Since GSH capping influences the sizes of synthesized NPs/NCs, no study compared the antimicrobial activity of GSH-capped NPs/NCs with those of uncapped NPs/NCs. Furthermore, no study was reported about GSH treatment on bulk copper and its alloys for the enhancement of their antimicrobial activity except our approach.<sup>35</sup>

Several research groups studied addition of a reducing agent to testing solution to enhance the antibacterial activity of copper salts or NPs.<sup>30,32,36</sup> Ojaim et al. reported that the addition of extra ascorbic acid (VC) to VC-capped copper NPs enhanced their antibacterial activity against *Staphylococcus aureus* and *Pseudomonas aeruginosa* due to an increase in ROS generation inside the bacterial cells.<sup>30</sup> GSH also has reducing activity reacting with copper ions, which may result in increasing ROS generation as shown in eqs 1–3. When copper and its alloys were immersed in 1/500 NB containing 1 mM GSH for 24 h, the generation of H<sub>2</sub>O<sub>2</sub> was detected in all tested materials<sup>35</sup> (Figure S8).

In the present study, EIS of the specimen with/without GSH treatment under a thin electrolyte was measured to investigate the acceleration of corrosion by the GSH treatment at a condition mimicking the bacteriophage contact in the antiviral assay. Figure 3 suggests the acceleration effect of GSH on corrosion at relatively high humidity such as 90% RH and in an electrolyte (100%). Figure 3b also suggests the trend in the effect of the GSH treatment depending on Cu content in the alloys; the higher Cu content tends to have the higher enhancement effect. Figure 4a and Figure S7a revealed the correlation tendency between the corrosion rate ( $1/Z_{\text{diff}}$ ) and antiviral activities ( $T_{0.001}$  and MICT) with the GSH treatment except MONEL, suggesting the importance of the corrosion rate on antiviral activity. It is also confirmed by the correlation tendency between the enhancement levels in antiviral activity and those in corrosion rates except C5191, as shown in Figure 4a and Figure S7b. Even with a few exceptions, these data suggest the dependent tendency of the antiviral activity of testing materials on their corrosion rates. Copper antimicrobial activity is mainly attributed to released copper ions and related reactions such as ROS generation.<sup>5,17,18</sup> The involvement of copper ions in their antibacterial activity is confirmed by Cu accumulation inside the bacterial cells in contact with the copper surface.<sup>37</sup> Our previous study<sup>22</sup> also reported the importance of the corrosion rate on copper antibacterial activity; retardation in the corrosion rate under a low-humidity environment contributed to reduction



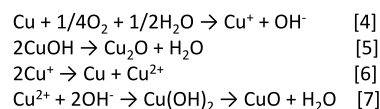
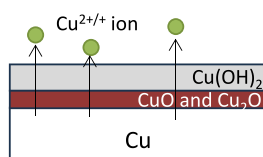
in copper antimicrobial activity. For Cu–Ni alloys, the increase in Ni content decreases the corrosion rate of the alloy in neutral NaCl solution,<sup>38</sup> which agrees with the results of this study; MONEL has a lower corrosion rate than C7150 and Constantan (Figure 3a). The surface analysis of MONEL exposed in ambient conditions revealed the formation of Ni(OH)<sub>2</sub> together with Cu<sub>2</sub>O;<sup>39</sup> the former is the main composition of the Ni passivity film.<sup>40</sup> Cu–Ni alloys with higher Cu content lose the benefit of Ni passivity, showing the corrosion behavior similar to Cu.<sup>41</sup> When Cu–66 wt % Ni–2 wt % Fe and Cu–23 wt % Ni–12 wt % Zn–2.5 wt % Sn alloys were immersed into synthetic sweat, Ni compounds were found in the corrosion products of the former, but not of the latter,<sup>42</sup> suggesting the Ni ion release from the high-Ni-content alloy. Ni has antimicrobial activity but is much lower than that of Cu.<sup>43</sup> These will explain the lower corrosion acceleration of MONEL by GSH treatment as well as its lower antiviral activity than other copper alloys.

The mechanism of how GSH accelerates copper corrosion can be explained by the change in the surface oxide thickness. As shown in Figure 5 and Table 2, the thickness of surface oxide on C1020 was slightly reduced after GSH treatment. The surface oxide formation on C1020 contributes to slowing down the diffusion of oxygen at the surface, retarding the corrosion reaction of Cu. Therefore, the thinning of the oxide layer reduces this

retardation, resulting in relatively faster corrosion. The GSH reaction with copper surface oxide may require H<sub>2</sub>O, as suggested by Figure 1b; the applied solution with lower H<sub>2</sub>O content is more effective for the enhancement of antiviral activity. Since GSH is insoluble in EtOH, the treatment solution must contain H<sub>2</sub>O to dissolve GSH. However, the presence of H<sub>2</sub>O helps Cu(OH)<sub>2</sub> formation at the copper surface, which is relatively fast in a humid atmosphere.<sup>27</sup> The GSH treatment solution with low H<sub>2</sub>O content has two possible roles to minimize the Cu(OH)<sub>2</sub> formation; one is simple minimization of the Cu(OH)<sub>2</sub> formation by low H<sub>2</sub>O content, and the other is inhibition of the Cu(OH)<sub>2</sub> formation via reduction of Cu<sup>2+</sup> to Cu<sup>+</sup> by GSH as shown in eq 1. The latter role would be important to describe the results in the present study. C1020 treated with 99 vol % EtOH without GSH has slightly increased its antiviral activity at a short contact time in comparison to nontreated C1020 as shown in Figure 1a, while GSH-treated C1020 indicated better antiviral activities than the nontreated one as shown in Figure 1b and Figure S4. These results cannot determine the dominance between the following processes for antiviral activity: ROS generation by Cu<sup>+</sup> reaction with O<sub>2</sub>/H<sub>2</sub>O<sub>2</sub> (eqs 2 and 3) or corrosion acceleration by thinning of the Cu(OH)<sub>2</sub> layer. In either of them, GSH contributed via reduction of Cu<sup>2+</sup> to Cu<sup>+</sup>.

The influence of GSH treatment on the copper surface is schematically described in Figure 6. The nontreated copper

(a) No treatment



(b) GSH treatment

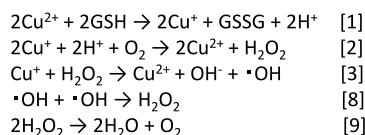
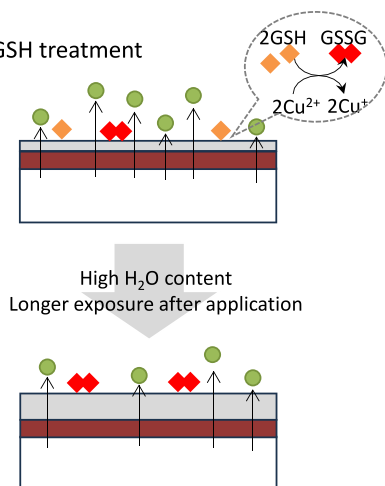
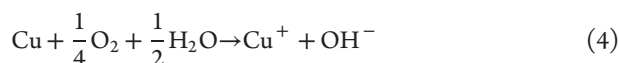
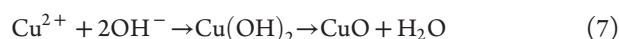


**Figure 6.** Schematic illustration of the effect of GSH treatment on the oxide layer of the copper surface and its corrosion resistance. (a) In the case of no treatment, copper corrosion occurs as shown in eq 4, forming Cu<sub>2</sub>O via CuOH (eq 5). In high concentrations, Cu<sup>+</sup> will disproportionate into Cu and Cu<sup>2+</sup>, which contributes to form CuO via Cu(OH)<sub>2</sub> (eqs 6 and 7). (b) In the case of GSH treatment, GSH reduces Cu<sup>2+</sup> to Cu<sup>+</sup> (eq 1), which will go through the disproportionation and decrease oxide formation. Cu<sup>+</sup> also contributes to the generation of ROS such as H<sub>2</sub>O<sub>2</sub> and  $\cdot\text{OH}$  in the presence of H<sup>+</sup> (eqs 2 and 3), which can give extra damage to viruses and microbiomes when they are challenged on the copper surface. However, their lifetime is relatively short due to their decomposition (eqs 8 and 9). At the long exposure time after the treatment, all the GSH applied to the copper surface is consumed by the reaction shown in eq 1; the thickness of the surface oxide layer increases again. This decreases the release of Cu<sup>2+</sup>/Cu<sup>+</sup> ions, resulting in a decrease in their antiviral/antibacterial activity.

surface is naturally oxidized via CuOH formation in the following equations:<sup>44</sup>



With an increase in its concentration,  $\text{Cu}^+$  goes through disproportionation into Cu and  $\text{Cu}^{2+}$ , in which the latter contributes to form CuO via  $\text{Cu}(\text{OH})_2$  by the following equations.<sup>44</sup>



On the GSH-treated surface, besides the reactions described above, GSH reduces  $\text{Cu}^{2+}$  to  $\text{Cu}^+$  (eq 1), which goes through the disproportionation (eq 5), resulting in decrease of oxide formation.  $\text{Cu}^+$  also contributes to the generation of ROS such as  $\text{H}_2\text{O}_2$  and  $\cdot\text{OH}$  in the presence of  $\text{H}^+$  (eqs 2 and 3), which can give extra damage to viruses and bacteria when they are in contact with the copper surface. However, the lifetime of ROS is relatively short due to their decomposition.



This means that the only ROS generated “in situ”—very close to the pathogens—can give damage to them. The  $\text{Cu}^{2+}$  reduction by GSH (eq 1) consumes GSH, which decreases the remaining GSH on the surface with an increase in exposure time. Therefore, at a long exposure after the treatment, all the GSH applied to the copper surface is consumed by the reaction of eq 1 and the thickness of the surface oxide layer increases again. This also decreases the release of  $\text{Cu}^+$  ions, resulting in a decrease in their antiviral/antibacterial activity. Figure S5 confirms that the long exposure of 168 h after the treatment decreased the antiviral activity of the GSH-treated C1020 to the same level to that of the nontreated one, though the contact time of the nontreated one was doubled.

The difference in the effectiveness of the GSH treatment among testing materials can be derived from the difference in surface oxide thickness and composition, resulting in different influences on corrosion reaction. The corrosion acceleration is more obvious on high-Cu-content alloys than low-Cu-content alloys (Figure 3b), suggesting that the incorporation of alloying elements in surface oxide influences the effect of the GSH treatment. Further investigation is necessary to clarify the roles of alloying elements in surface oxide and the GSH treatment.

The developed GSH treatment is simple and easily applicable to copper high touch surfaces when needed, in such a way as an alcohol disinfectant. This treatment has the following advantages: (1) GSH is widely distributed in mammalian cells, expecting low toxicity to animals. (2) A water–ethanol system is employed as a solvent, which can be applicable like other alcoholic disinfectants. (3) There is no need for heat treatment nor a specific equipment for application. Since we tested with a small specimen, we just dropped a small portion of the treatment solution onto the specimen surface, but it is possible to

apply by spraying to a large surface. This also allows the application to existing touch surfaces. (4) Since the GSH treatment mainly works to reduce the natural oxide thickness, damage to the copper materials is limited. Therefore, it enables repetitive application. When the treated surface receives mechanical wear or chemical cleaning, it can be applied again to the surface.

The limitation of this treatment is the duration of its effect shorter than 7 days, which requires a repetitive application. The exposure of the treated surface was performed in a laboratory environment at ambient temperature and humidity around 50% RH, which is a relatively mild, indoor atmosphere. A higher temperature and humidity may accelerate copper oxide formation, which accelerates consumption of GSH, resulting in shorter duration of the treatment effect. Furthermore, the antiviral assay is performed in laboratory conditions; bacteriophage Q $\beta$  suspension is applied to the specimen surface with a polyethylene film, making a thin suspension layer, keeping it moist through the contact time. In practical conditions, however, pathogen contact to high touch surfaces is mainly by a droplet, which dries relatively fast under ambient conditions. The GSH treatment accelerates copper corrosion markedly at 100% RH, but it decreases in low-humidity conditions. This suggests that GSH requires  $\text{H}_2\text{O}$  for thinning the surface oxide layer and that the improvement in the antimicrobial effect by this treatment may be reduced in a practical, less humid environment than that obtained in a laboratory. In this study, the GSH influence on the oxide layer of the copper surface was investigated by electrochemical methods. Further investigation with detailed analysis of the oxide layer by X-ray photoelectron spectroscopy or other methods is necessary to deeply understand the durability and efficacy of the GSH treatment with different copper materials.

## 5. CONCLUSIONS

We attempted a surface treatment of copper to enhance its antiviral activity, which is evaluated using bacteriophage Q $\beta$ , a nonenveloped virus. Treatment of copper and its alloy surface with 4 mM GSH in 99 vol % EtOH distinctly enhanced their antiviral activity except MONEL, the Ni-33.4 wt % Cu alloy.

Electrochemical impedance measurement of the testing materials revealed the significant acceleration in their corrosion rates by the GSH treatment for C1020, C7150, and Constantan, while the increase in those of C5191 and C2680 was not statistically significant. The antiviral activity of testing materials with the treatment correlates well to their corrosion rate with the treatment except MONEL, suggesting the involvement of Ni passivity. The enhancement level in their antiviral activity by the treatment tends to correlate to the acceleration level in their corrosion rates. Potentiodynamic and chronopotentiometric measurement confirmed the reduction of copper surface oxide by the treatment, suggesting its contribution to the acceleration of corrosion.

Most of copper alloys have higher stability against discoloration than C1020, but their antibacterial/antiviral activity is lower than C1020. The GSH treatment improved the antiviral activity of C5191, C2680, and Constantan to the level superior to nontreated C1020, which may encourage the touch surface application of copper alloys.

## ■ ASSOCIATED CONTENT


### Supporting Information

The Supporting Information is available free of charge at <https://pubs.acs.org/doi/10.1021/acsabm.6c00520>.

(Table S1) Chemical compositions of testing materials, (Table S2) statistical analysis applied to the pair of the results in different treatment solutions and materials obtained by the antiviral assay, (Figure S1) schematic explanation of the specimen for electrochemical impedance measurement, (Figure S2) schematic illustration of the antiviral assay, (Figure S3) equivalent circuit model, (Figure S4) effect of the concentrations of GSH, (Figure S5) effect of the leaving time, (Figure S6) typical examples for the results of electrochemical impedance measurement, (Figure S7) correlation between MICT and  $1/Z_{\text{diff}}$  and (Figure S8)  $\text{H}_2\text{O}_2$  generation after 24 h of immersion (PDF)

## AUTHOR INFORMATION

### Corresponding Author

Akiko Yamamoto – Research Center for Macromolecules and Biomaterials, National Institute for Materials Science, 1-1 Namiki, Tsukuba, Ibaraki 305-0044, Japan;  0000-0002-9182-4886; Email: YAMAMOTO.Akiko@nims.go.jp. Tel.: +81-29-860-4169. Fax: +81-29-860-4626

### Authors

Masanori Kikuchi – Bioceramics Group, Research Center for Macromolecules and Biomaterials, National Institute for Materials Science, 1-1 Namiki, Tsukuba, Ibaraki 305-0044, Japan

Yasushi Suetsugu – Bioceramics Group, Research Center for Macromolecules and Biomaterials, National Institute for Materials Science, 1-1 Namiki, Tsukuba, Ibaraki 305-0044, Japan

Complete contact information is available at:

<https://pubs.acs.org/doi/10.1021/acsabm.6c00520>

### Author Contributions

Conceptualization, A.Y.; data curation, A.Y.; formal analysis, A.Y.; funding acquisition, A.Y. and M.K.; methodologies, A.Y.; project administration, A.Y. and M.K.; resources, A.Y. and M.K.; supervision, A.Y. and M.K.; validation, Y.S. and M.K.; visualization, A.Y.; writing-original draft, A.Y.; writing-review and editing, Y.S. and M.K. All authors have given approval to the final version of the manuscript.

### Funding

This work was partially supported by JST A-STEP (Grant Number JPMJTM20KSPS), Japan.

### Notes

The authors declare no competing financial interest.

## ACKNOWLEDGMENTS

The authors appreciate Ms. Masuko Tsuda and Ms. Akemi Kikuta from NIMS for their technical assistance on antiviral tests and electrochemical impedance measurements.

## ABBREVIATIONS

VRE vancomycin-resistant Enterococci  
HAI healthcare-associated infection  
ICU intensive care unit

DNA deoxyribonucleic acid  
UV ultraviolet  
JIS Japanese Industrial Standard  
C1020 oxygen-free copper  
C5190 Cu-6.5 wt % Sn alloy  
C7150 Cu-30 wt % Ni alloy  
C2680 Cu-35% Zn alloy  
MONEL MONEL400, Ni-30 wt % Cu alloy  
GSH glutathione  
EtOH ethanol  
LB Luria–Bertani broth  
CaLB LB-supplemented calcium salt  
pfu plaque-forming unit  
NB nutrient broth  
SCDLP soybean-casein digest broth with lecithin and polyoxyethylene sorbitan monooleate  
 $N$  virus infectivity titer  
 $A$  average number of plaques in the duplicated dishes at the same dilution  
 $D_F$  dilution factor  
 $V$  volume of the bacteriophage suspension added to the *E. coli* suspension  
 $N_{\text{mat}}$   $N$  on the specimen surface  
 $N_{\text{cont}}$   $N$  on the control surface  
 $T_{0.001}$  contact time to reduce  $N_{\text{mat}}$  to 1/1000 of  $N_{\text{cont}}$   
MICT minimum inhibitive contact time  
EIS electrochemical impedance spectroscopy  
RH relative humidity  
 $Z_{\text{high}}$  the impedance at high frequency range  
 $Z_{\text{low}}$  the impedance at low frequency range  
 $R_s$  the sum of electric resistance of the electrolyte  
 $R_c$  charge transfer resistance  
 $Z_{\text{diff}}$  the difference between  $Z_{\text{high}}$  and  $Z_{\text{low}}$   
 $I_{\text{corr}}$  corrosion rate (corrosion current density)  
 $k_a$  constant  
 $k'_a$  constant  
PD potentiodynamic  
CP chronopotentiometric  
GSH\_99 4 mM GSH in 99 vol % EtOH + 1 vol %  $\text{H}_2\text{O}$

## REFERENCES

- (1) Mitchell, B. G.; Dancer, S. J.; Anderson, M.; Dehn, E. Risk of Organism Acquisition from Prior Room Occupants: A Systematic Review and Meta-Analysis. *J. Hosp. Infect.* **2015**, *91*, 211–217.
- (2) Marra, A. R.; Schweizer, M. L.; Edmond, M. B. No-Touch Disinfection Methods to Decrease Multidrug-Resistant Organism Infections: A Systematic Review and Meta-Analysis. *Infect. Control Hosp. Epidemiol.* **2018**, *39*, 20–31.
- (3) van der Starre, C. M.; Cremers-Pijpers, S. A. J.; van Rossum, C.; Bowles, E. C.; Tostmann, A. The in situ Efficacy of Whole Room Disinfection Devices: a Literature Review with Practical Recommendations for Implementation. *Antimicrob. Resist. Infect. Control* **2022**, *11*, No. 149.
- (4) Carling, P. C.; O'Hara, L. M.; Harris, A. D.; Olmsted, R. Mitigating Hospital-Onset *Clostridioides difficile*: The Impact of an Optimized Environmental Hygiene Program in Eight Hospitals. *Infect. Control Hosp. Epidemiol.* **2023**, *44*, 440–446.
- (5) Grass, G.; Rensing, C.; Solioz, M. Metallic Copper as an Antimicrobial Surface. *Appl. Environ. Microbiol.* **2011**, *77*, 1541–1547.
- (6) Michels, H. T.; Michels, C. A. Copper Alloys — The New 'Old' Weapon in the Fight Against Infectious Disease. *Curr. Trends Microbiol.* **2016**, *10*, 23–45.



- (7) Vincent, M.; Duval, R. E.; Hartemann, P.; Engels-Deutsch, M. Contact Killing and Antimicrobial Properties of Copper. *J. Appl. Microbiol.* **2017**, *124*, 1032–1046.
- (8) Wang, Y.; Li, H.; Yuan, X.; Jiang, Y.; Xiao, Z.; Li, Z. Review of Copper and Copper Alloys as Immune and Antibacterial Element. *Trans. Nonferrous Met. Soc. China* **2022**, *32*, 3163–3181.
- (9) Dauvergne, E.; Mullié, C. Brass Alloys: Copper-Bottomed Solutions against Hospital-Acquired Infections? *Antibiotics* **2021**, *10*, No. 286.
- (10) Pineda, I.; Hubbard, R.; Rodríguez, F. The role of copper surfaces in reducing the incidence of healthcare-associated infections: A systematic review and meta-analysis. *Can. J. Infect. Control* **2017**, *32* (1).
- (11) Salgado, C. D.; Sepkowitz, K. A.; John, J. F.; Cantey, J. R.; Attaway, H. H.; Freeman, K. D.; Sharpe, P. A.; Michels, H. T.; Schmidt, M. G. Copper Surfaces Reduce the Rate of Healthcare-Acquired Infections in the Intensive Care Unit. *Infect. Control Hosp. Epidemiol.* **2013**, *34*, 479–486.
- (12) Schmidt, M. G.; von Dessauer, B.; Benavente, C.; Benadof, D.; Cifuentes, P.; Elgueta, A.; Duran, C.; Navarrete, M. S. Copper Surfaces are Associated with Significantly Lower Concentrations of Bacteria on Selected Surfaces within a Pediatric Intensive Care Unit. *Am. J. Infect. Control* **2016**, *44*, 203–209.
- (13) von Dessauer, B.; Navarrete, M. S.; Benadof, D.; Benavente, C.; Schmidt, M. G. Potential Effectiveness of Copper Surfaces in Reducing Health Care-Associated Infection Rates in a Pediatric Intensive and Intermediate Care Unit: A Nonrandomized Controlled Trial. *Am. J. Infect. Control* **2016**, *44*, e133–e139.
- (14) Hinsla-Leasure, S. M.; Nartey, Q.; Vaverka, J.; Schmidt, M. G. Copper Alloy Surfaces Sustain Terminal Cleaning Levels in a Rural Hospital. *Am. J. Infect. Control* **2016**, *44*, e195–e203.
- (15) Suzuki, S.; Ishikawa, Y.; Isshiki, M.; Waseda, Y. Native Oxide Layers Formed on the Surface of Ultra High-Purity Iron and Copper Investigated by Angle Resolved XPS. *Mater. Trans., JIM* **1997**, *38*, 1004–1009.
- (16) Yamamoto, A.; Tanaka, S.; Ohishi, K. Quantitative Evaluation of Nucleic Acid Degradability of Copper Alloy Surfaces and Its Correlation to Antibacterial Activity. *Antibiotics* **2021**, *10*, No. 1439.
- (17) Quaranta, D.; Krans, T.; Santo, C. E.; Elowsky, C. G.; Domaille, D. W.; Chang, C. J.; Grass, G. Mechanisms of Contact-Mediated killing of Yeast Cells on Dry Metallic Copper Surfaces. *Appl. Environ. Microbiol.* **2011**, *77*, 416–426.
- (18) Hans, M.; Mathews, S.; Mucklich, F.; Solioz, M. Physicochemical Properties of Copper Important for its Antibacterial Activity and Development of a Unified Model. *Biointerphases* **2016**, *11*, No. 018902.
- (19) Hans, M.; Erbe, A.; Mathews, S.; Chen, Y.; Solioz, M.; Mücklich, F. Role of Copper Oxides in Contact Killing of Bacteria. *Langmuir* **2013**, *29*, 16160–16166.
- (20) Watanabe, B.; Hiratake, J. Glutathione Metabolism and Thiol Chemistry. *Kagaku to Seibutsu* **2015**, *53*, 354–361.
- (21) JIS R1706:2020 Fine Ceramics (Advanced Ceramics, Advanced Technical Ceramics) — Determination of Antiviral Activity of Photocatalytic Materials — Test Method Using Bacteriophage Q-beta.
- (22) Yamamoto, A.; Ito, Y. Effect of Humidity on Antibacterial Activity of Copper and Its Alloy Surfaces. *Mater. Trans.* **2026**, *67*, 83–91.
- (23) Katayama, H. Electrochemical Measurements in Various Environments—Atmospheric Corrosion II (Electrochemical Impedance Method)—. *Zairyo to Kankyo* **2018**, *67* (7), 280–286.
- (24) Katayama, H.; Noda, K.; Yamamoto, M.; Kodama, T. Relationship between Corrosion Rate of Carbon Steel and Water Film Thickness under Thin Layer of Artificial Sea Water. *J. Japan Inst. Metals* **2001**, *65*, 298–302.
- (25) Nakayama, S.; Kaji, T.; Shibata, M.; Notoya, T.; Osakai, T. Which is Easier to Reduce, Cu<sub>2</sub>O or CuO? *J. Electrochem. Soc.* **2007**, *154* (1), C1–C6.
- (26) Walkowicz, M.; Osuch, P.; Smyrak, B.; Knych, T.; Rudnik, E.; Cieniek, Ł.; Różańska, A.; Chmielarczyk, A.; Romaniszyn, D.; Bulanda, M. Impact of Oxidation of Copper and its Alloys in Laboratory-Simulated Conditions on Their Antimicrobial Efficiency. *Corros. Sci.* **2018**, *140*, 321–332.
- (27) Nakayama, S.; Notoya, T.; Osakai, T. A Mechanism for the Atmospheric Corrosion of Copper Determined by Voltammetry with a Strongly Alkaline Electrolyte. *J. Electrochem. Soc.* **2010**, *157*, C289–C294.
- (28) Rowan, N. J.; Kremer, T.; McDonnell, G. A Review of Spaulding's Classification System for Effective Cleaning, Disinfection and Sterilization of Reusable Medical Devices: Viewed through a Modern-Day Lens that will Inform and Enable Future Sustainability. *Sci. Total Environ.* **2023**, *878*, No. 162976.
- (29) Sahu, M.; Ganguly, M.; Doi, A. Role of Glutathione Capping on Copper Nanoclusters and Nanoparticles: A Review. *J. Cluster Sci.* **2024**, *35*, 1667–1685.
- (30) Ojaym, A.; Hillyer, T.; Chen, G.; Huang, S. D.; Shin, W. S.; Kim, M. H. Harnessing the Synergy of Copper Nanoparticles and Vitamin C towards the Resolution of Wound Infection. *Biomater. Sci.* **2025**, *13*, 5813–5824.
- (31) Sen, S.; Sarkar, K. Effective Biocidal and Wound Healing Cogeneity of Biocompatible Glutathione: Citrate-Capped Copper Oxide Nanoparticles against Multidrug-Resistant Pathogenic Enterobacteria. *Microb. Drug Resist.* **2021**, *24*, 616–627.
- (32) Holloway, A. C.; Gould, S. W. J.; Fielder, M. D.; Naughton, D. P.; Kelly, A. F. Enhancement of antimicrobial activities of whole and sub-fractionated white tea by addition of copper (II) sulphate and vitamin C against *Staphylococcus aureus*; a mechanistic approach. *BMC Complementary Altern. Med.* **2011**, *11*, No. 115.
- (33) Priyadharshan, M.; Karthikeyan, M.; Rajkumar, S.; Ragaey, M. M.; Sholkamy, E. N. Investigation of Structural, Optical, Morphological and Compositional Properties of Agglomerated CuMn<sub>2</sub>O<sub>4</sub> Nanoparticles for In Vitro Anticancer Activity Against MCF-7 Cell Lines. *J. Inorg. Organomet. Polym. Mater.* **2025**, *35*, 5408–5420.
- (34) Chanthee, S.; Santikunaporn, M.; Jirasangthong, J.; Asavatesanupap, C. Synthesis and antimicrobial studies of nano-copper doped carbon substrates; activated carbon, reduced graphene oxide, and carbon nanofiber. *J. Met., Mater. Miner.* **2022**, *32*, 68–74.
- (35) Yamamoto, A.; Oishi, K.; Tanaka, S. Surface treatment method for copper or copper alloy, surface treatment liquid for sterilizing copper or copper alloy and sterilization method using copper or copper alloy treated by said method. US 11535939B2, **2022**.
- (36) McCarrell, E. M.; Gould, S. W. J.; Fielder, M. D.; Kelly, A. F.; Sankary, W. E.; Naughton, D. P. Antimicrobial activities of pomegranate rind extracts: enhancement by addition of metal salts and vitamin C. *BMC Complementary Altern. Med.* **2008**, *8*, No. 64.
- (37) Santo, C. E.; Lam, E. W.; Elowsky, C. G.; Quaranta, D.; Domaille, D. W.; Chang, C. J.; Grass, G. Bacterial Killing by Dry Metallic Copper Surfaces. *Appl. Environ. Microbiol.* **2011**, *77*, 794–802.
- (38) Badawy, W. A.; Ismail, K. M.; Fathi, A. M. Effect of Ni Content on the Corrosion Behavior of Cu-Ni alloys in Neutral Chloride solutions. *Electrochim. Acta* **2005**, *50*, 3603–3608.
- (39) Zhu, Y.; Wang, J.; Liu, H.; Ren, P.; Yan, F. Effect of Dissolved Oxygen Content on Tribo-Corrosion Behavior of Monel 4000 Alloy in Seawater. *Metals* **2024**, *14* (1), No. 6.
- (40) Shimodaira, S. *Material Science of Corrosion and Protection*. AGNE Gijutsu Center, **1995**.
- (41) Uhlig, H. H.; Revie, R. W. *Corrosion and Corrosion Control*. ed., John Wiley & Sons, **1985** (Translated by Matsuda S.; Matsushima I., supervised by Okamoto G.; Sangyo Tosho Publishing, 1989, pp.1-434).
- (42) Colin, S.; Beche, E.; Berjoan, R.; Jolibois, H.; Chambaudet, A. An XPS and AES Study of the Free Corrosion of Cu-, Ni- and Zn-Based Alloys in Synthetic Sweat. *Corros. Sci.* **1999**, *41*, 1051–1065.
- (43) Kawakami, H.; Yoshida, K.; Nishida, Y.; Kikuchi, Y.; Sato, Y. Antibacterial Properties of Metallic Elements for Alloying Evaluated with Application of JIS Z 2801:2000. *ISIJ Int.* **2008**, *48*, 1299–1304.
- (44) Tada, E.; Nishikata, A. Mechanism of Metal Corrosion. *Chem. Educ.* **2017**, *65*, 612–615.